Neuroscience 3200

Stuart and Redman, J Physiol, 1992 – Future Studies

https://doi.org/10.1113/jphysiol.1992.sp019023

https://physoc.onlinelibrary.wiley.com/doi/pdf/10.1113/jphysiol.1992.sp019023

https://39363.org/NOTES/WSU/2021/Spring/NEURO3200/MISC/StuartAndRedman.html

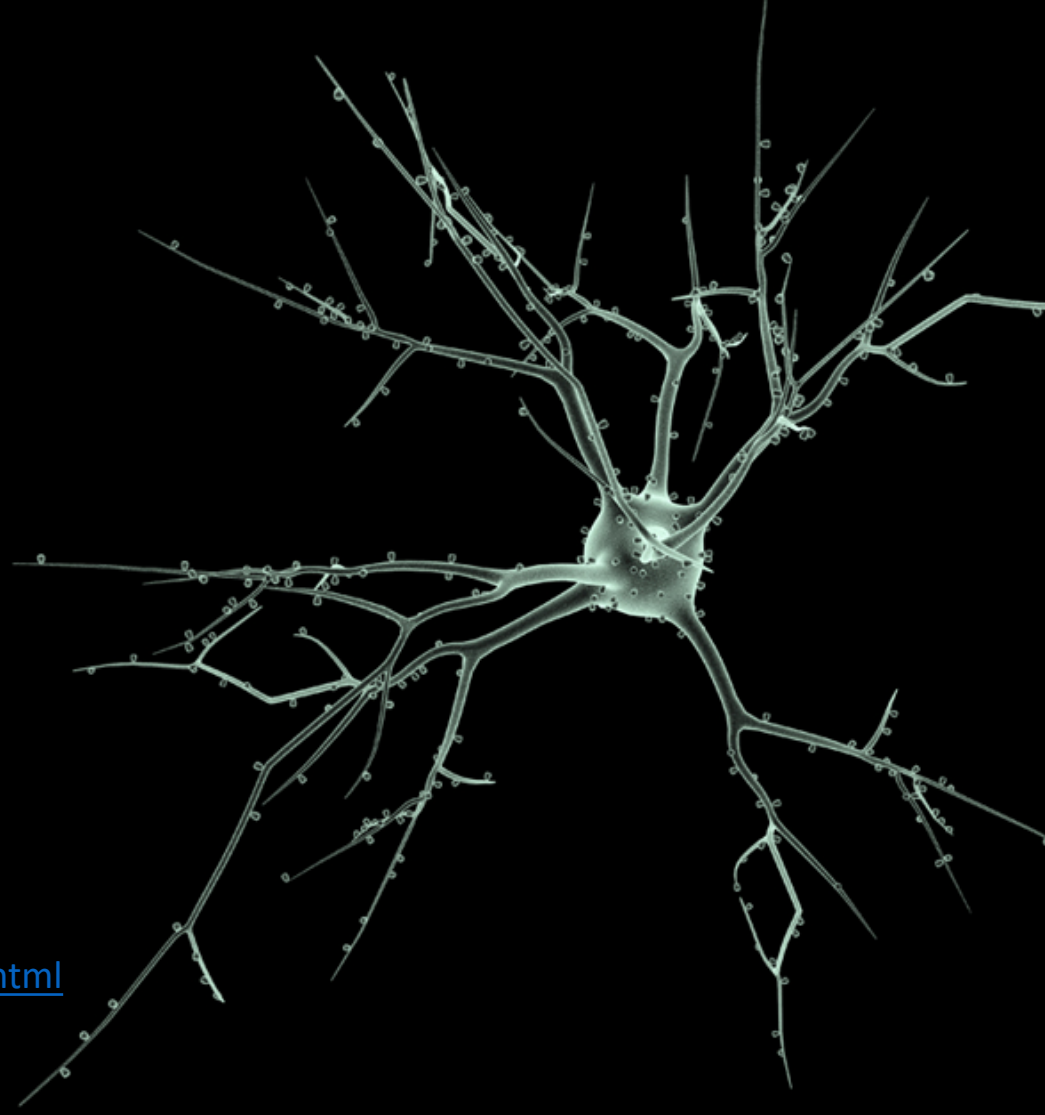

Presynaptic Inhibition

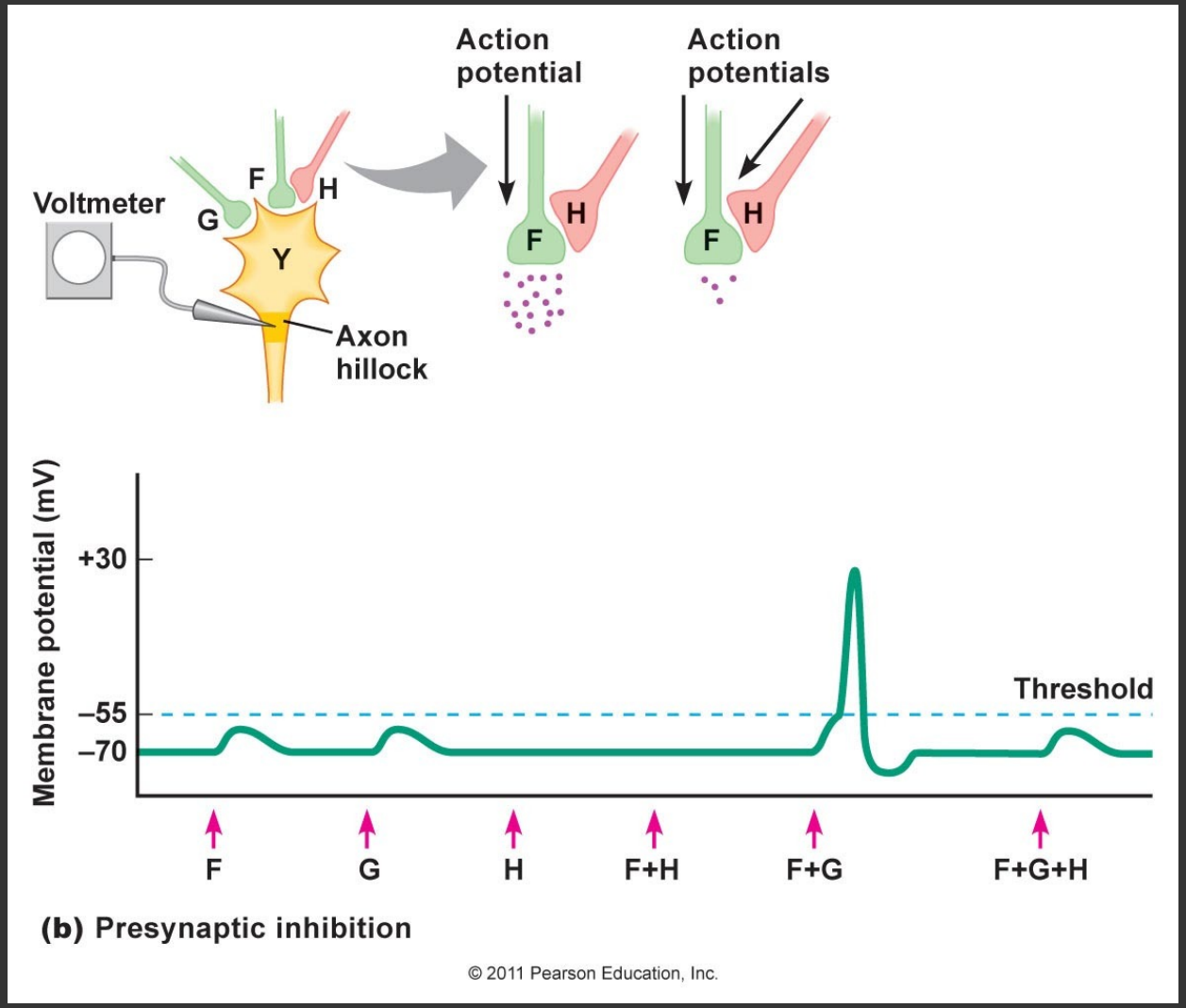

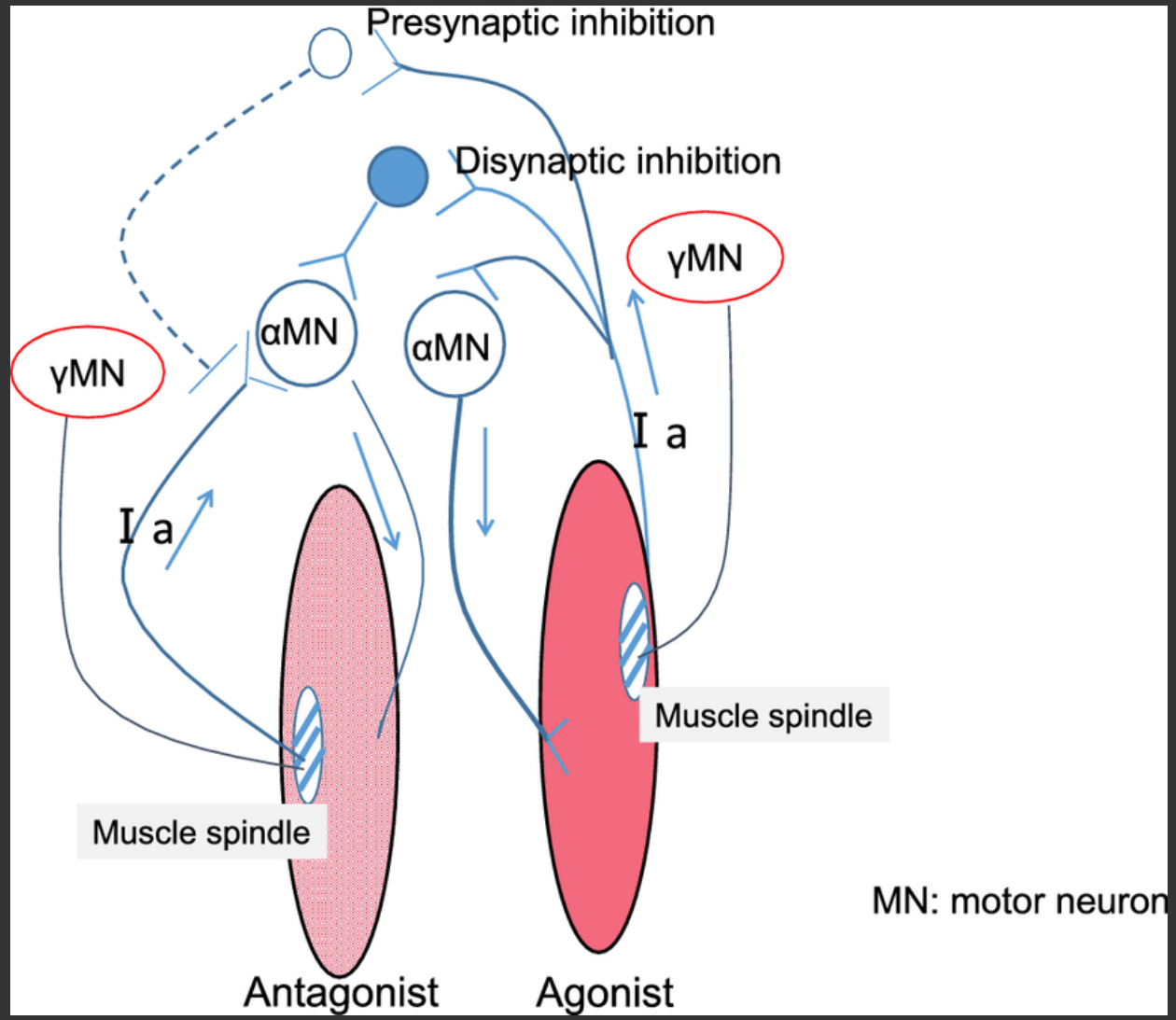

Presynaptic Inhibition

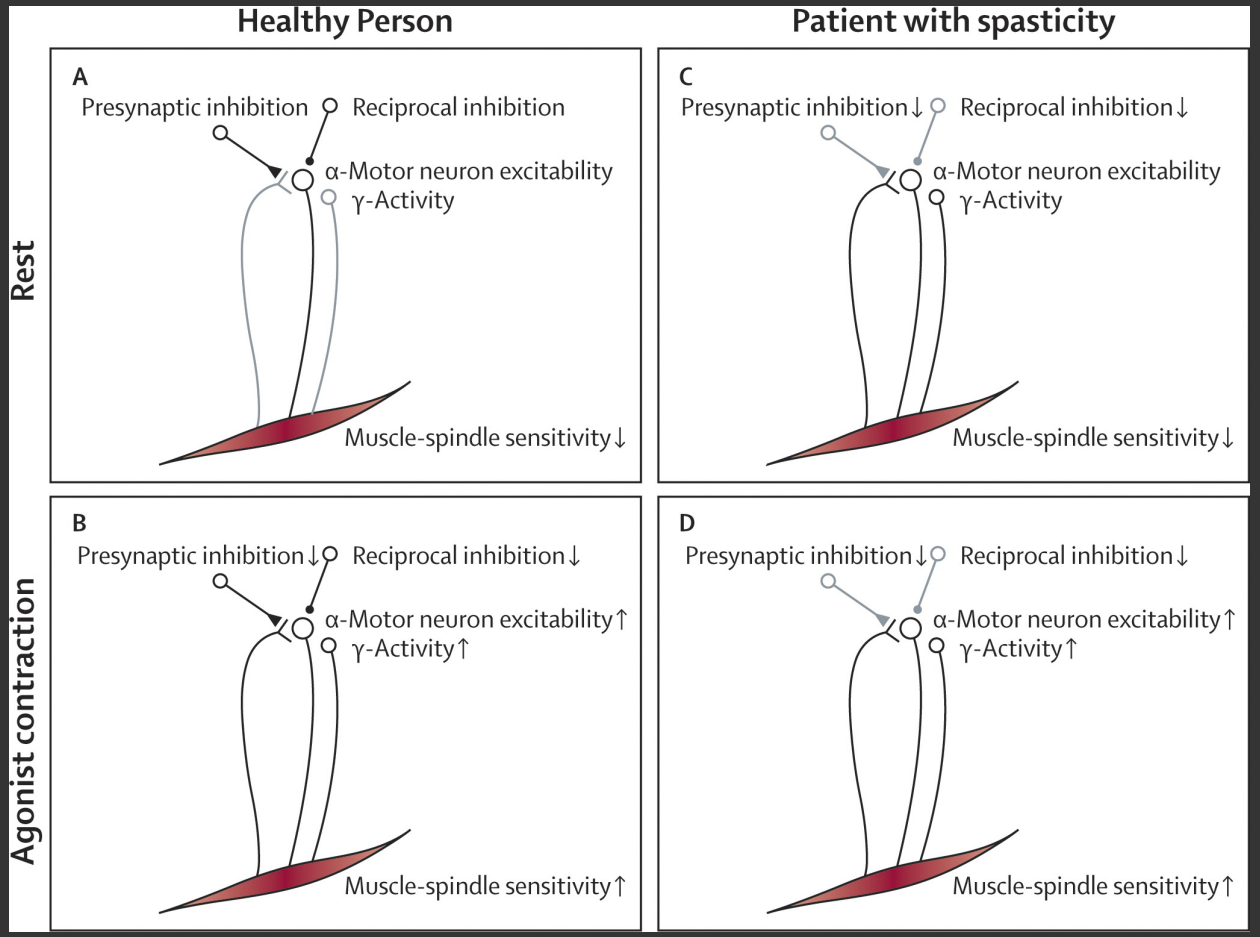

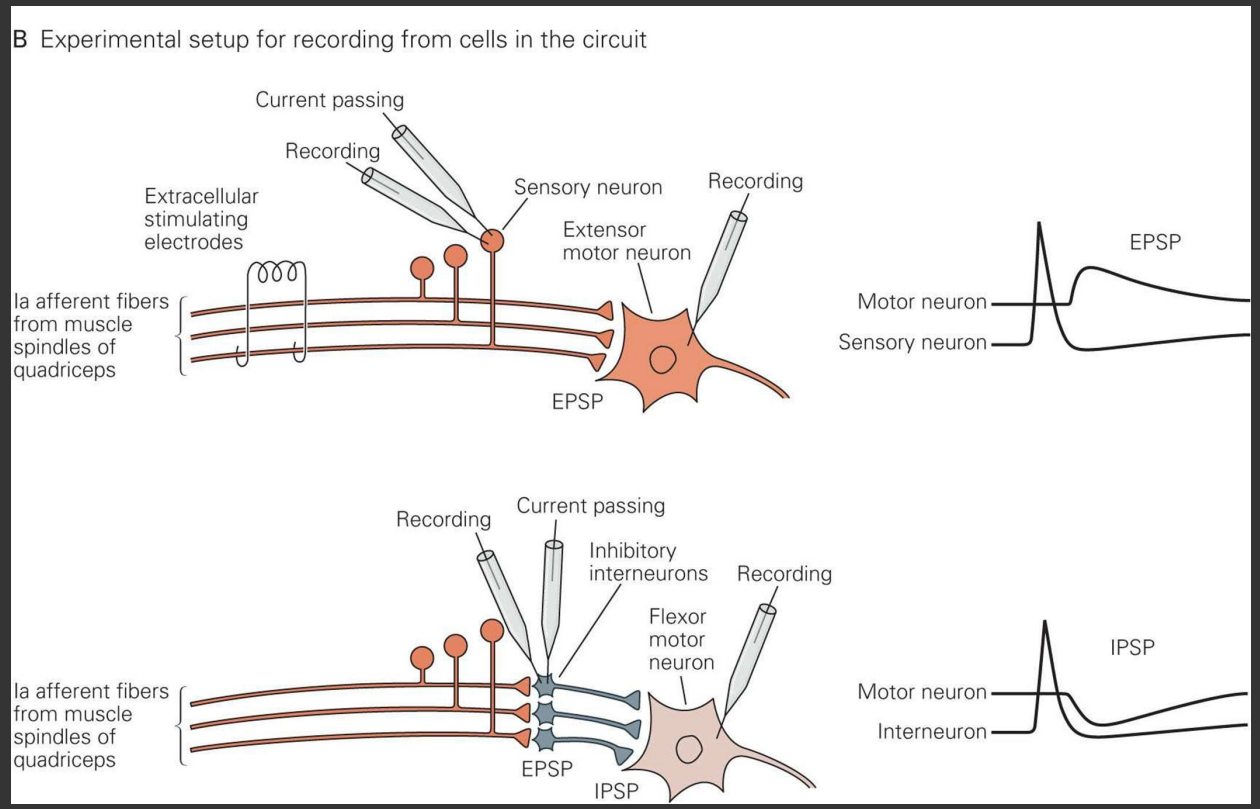

Presynaptic Inhibition

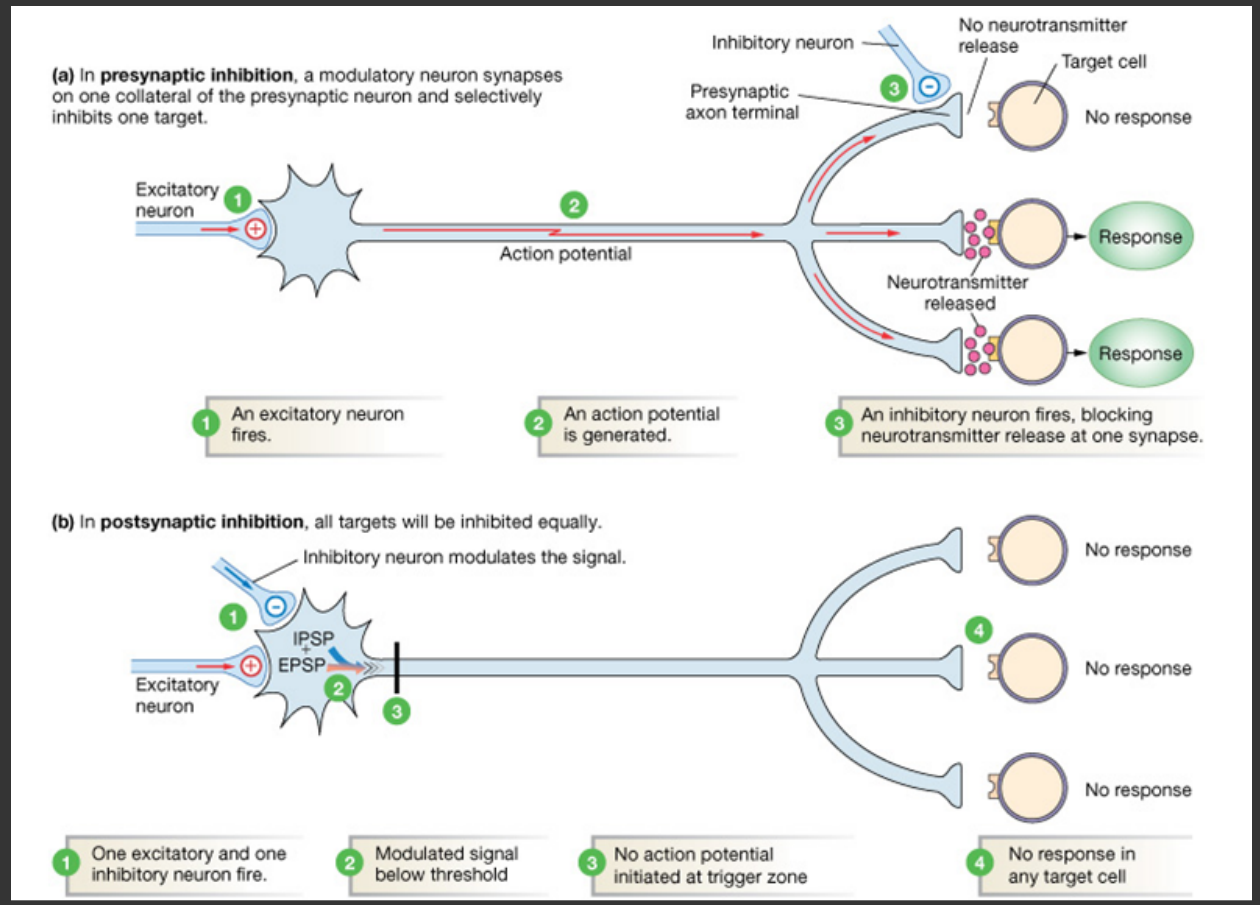

Renshaw cell inhibition

This phenomenon is called Renshaw cell inhibition (after Renshaw, who discovered it in 1946). The teleology of this phenomenon appears to be to produce a condition so that *even if the corticospinal tract fires repetitively*, the frequency of the muscle contraction remains less (Renshaw cell inhibition lasts for quite a few milli seconds), and thus the muscle is protected against too high frequency stimuli.

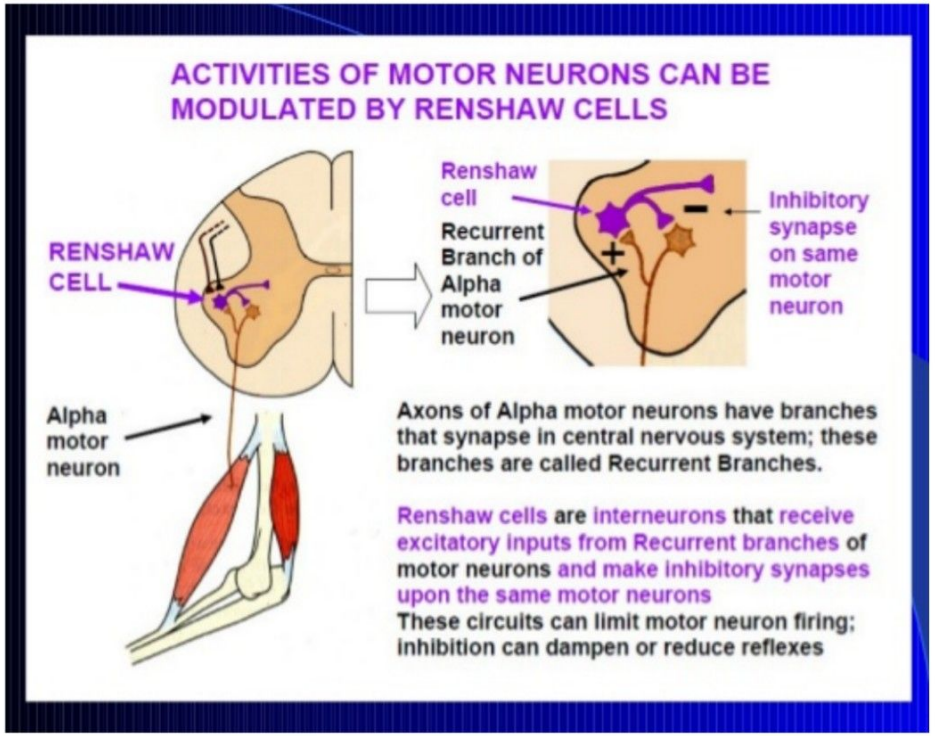

Goal

- The paper already proved that activation of $GABA_A$ receptors cause presynaptic inhibition
- We should try to find some other drug and or method by which we can discover another way presynaptic inhibition is mediated?

Targeting

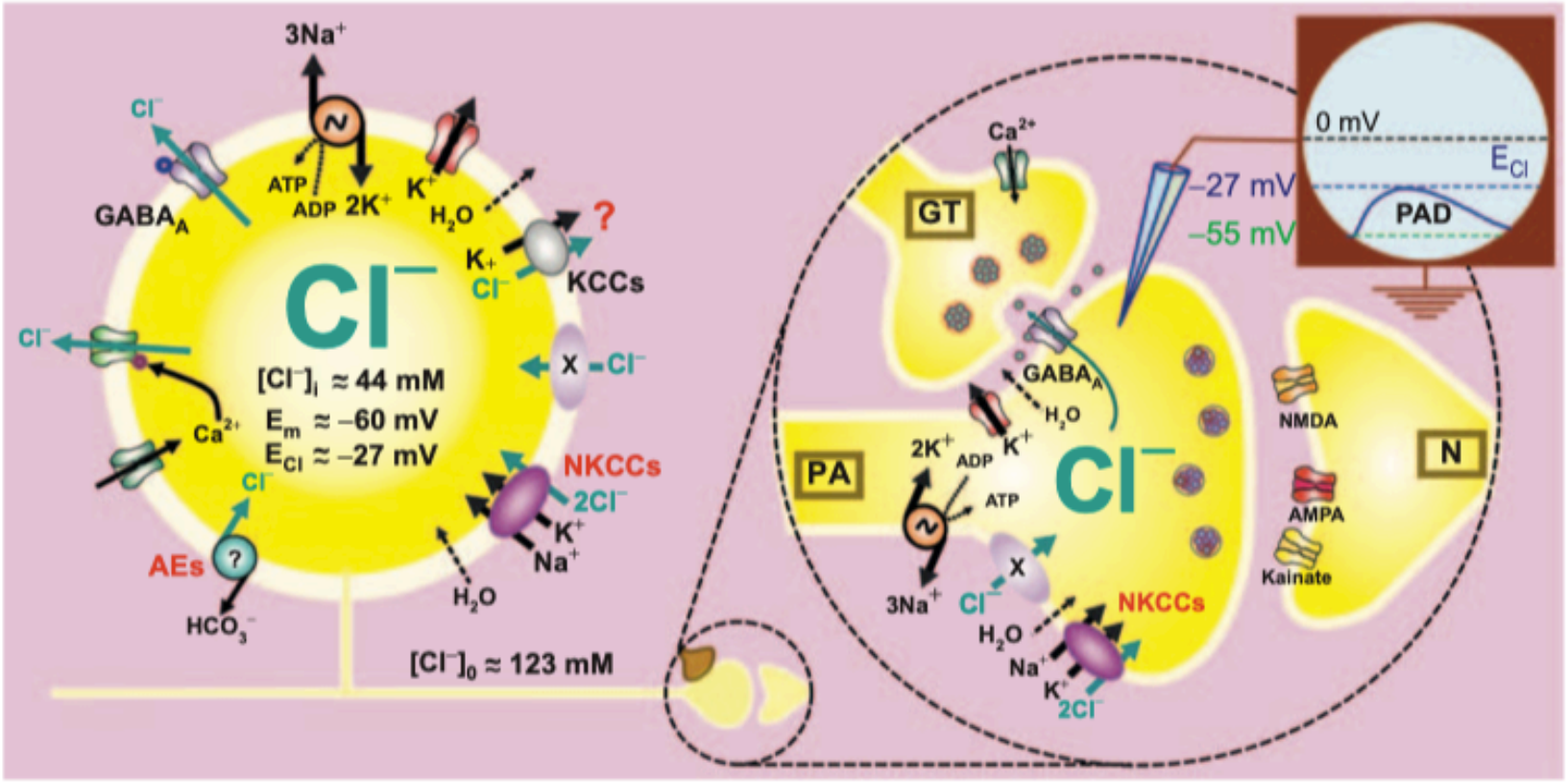

FIGURE 22.3 Schematic diagram depicting the known and hypothetical transporters and channels involved in intracellular Cl^- regulation in primary sensory neurons, and mode of generation of PAD and presynaptic inhibition. The left circle represents a DRG neuron showing measured values of intracellular Cl^- concentration, $[Cl^-]_i$; membrane potential (E_m) and Cl^- equilibrium potential, E_{Cl}. The Na^+/K^+ ATPase maintains the Na^+ and K^+ gradients across the membrane. AEs, anion exchangers; NKCCs, Na^+-K^+-$2Cl^-$ cotransporters and KCCs, are K^+-Cl^- cotransporters 1, 3 or 4 whose contribution, if any, to intracellular Cl^- regulation in these neurons under euvolemic conditions is not clear. KCC2 is not expressed in DRG neurons. X represents other yet to be identified active Cl^- uptake transporters. The right diagram encircled by a dashed line represents a magnified intraspinal primary afferent terminal from which an intracellular micropipette connected to an oscilloscope records E_m. PA, primary afferent; GT, GABAergic terminal from an interneuron; N, postsynaptic neuron with glutamate receptor channels. Note that PAD (blue trace in the oscilloscope screen) blocks the release of neurotransmitter from the PA terminal.

Targeting

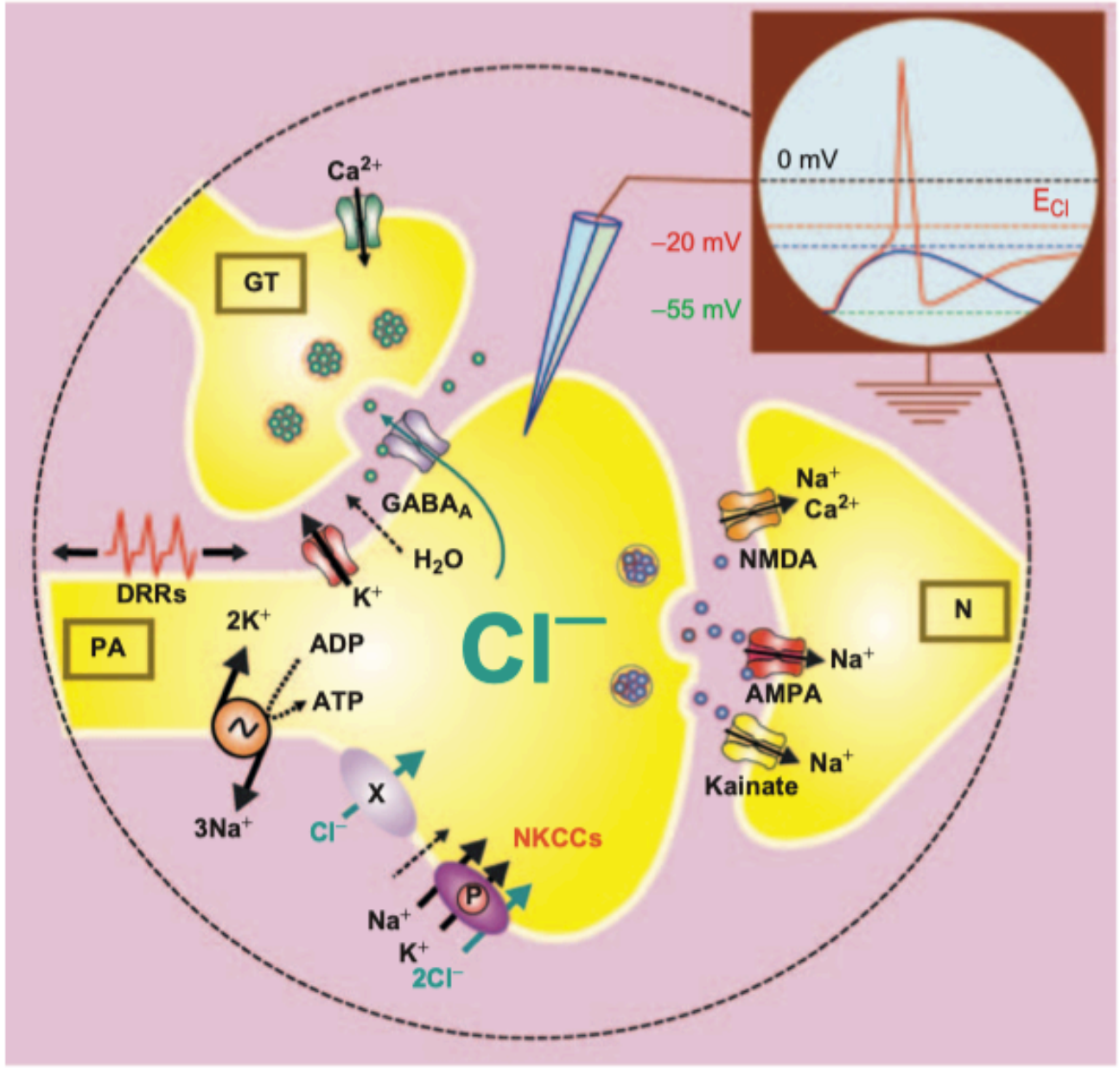

FIGURE 22.6 Schematic diagram illustrating the hypothesis of how activation of NKCCs and other yet to be identified active Cl^- uptake transport systems (X) increase $[Cl^-]_i$ in nociceptive presynaptic terminals (PA), shifting E_{Cl} toward depolarizing threshold values. Instead of PAD, GABA released from interneurons (GT) produces action potentials in the primary afferent (PA) terminals, as illustrated in the intracellular recording shown in the schematic representation of an oscilloscope screen. This results in dorsal root reflexes (DRRs) being conducted towards the periphery (antidromically) and towards the presynaptic terminal (orthodromically). The latter produces release of neurotransmitter from the presynaptic terminal, that activate the post-synaptic spinal neuron (N). Other symbols and nomenclature are the same as in the legend of Fig. 22.3.

Targeting

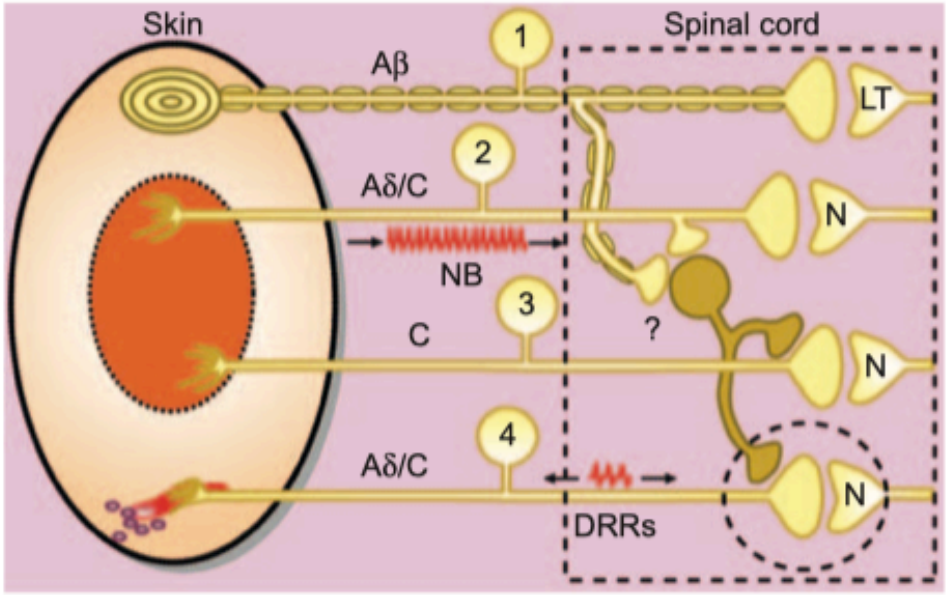

FIGURE 22.7 Hypothetical mechanisms of touch-evoked pain, hyperalgesia and neurogenic inflammation involving presynaptic interactions between primary sensory neurons. **Left oval**: skin patch with site of injury (orange) and surrounding uninjured area (peach). **Dashed rectangle**: dorsal horn with second order nociceptive neurons (N) and low threshold neurons (LT). Nociceptive barrage (NB) conducted through nociceptive primary afferent (cell 2). Dorsal root reflexes (DRRs). **Dashed circle** is magnified in Fig. 22.6. Under normal conditions, stimulation of low-threshold mechanoreceptors connected to Aβ afferents (cell 1) evokes PAD in the terminals of nociceptive afferents (Ao- and C fibers, cells 3 and 4) via GABAergic interneurons (mustard cell), reducing the effectiveness of nociceptive transmission. Following tissue injury and inflammation, the PAD evoked by tactile stimuli may become sufficiently large to evoke DRRs in nociceptive afferents. The DRRs conducted centripetally can excite neurons in the dorsal horn that are normally driven by nociceptors (N) and evoke mechanical allodynia. DRRs conducted centrifugally produce neurogenic inflammation (due to release of vasogenic mediators (cell 4) and hyperalgesia.

Targeting

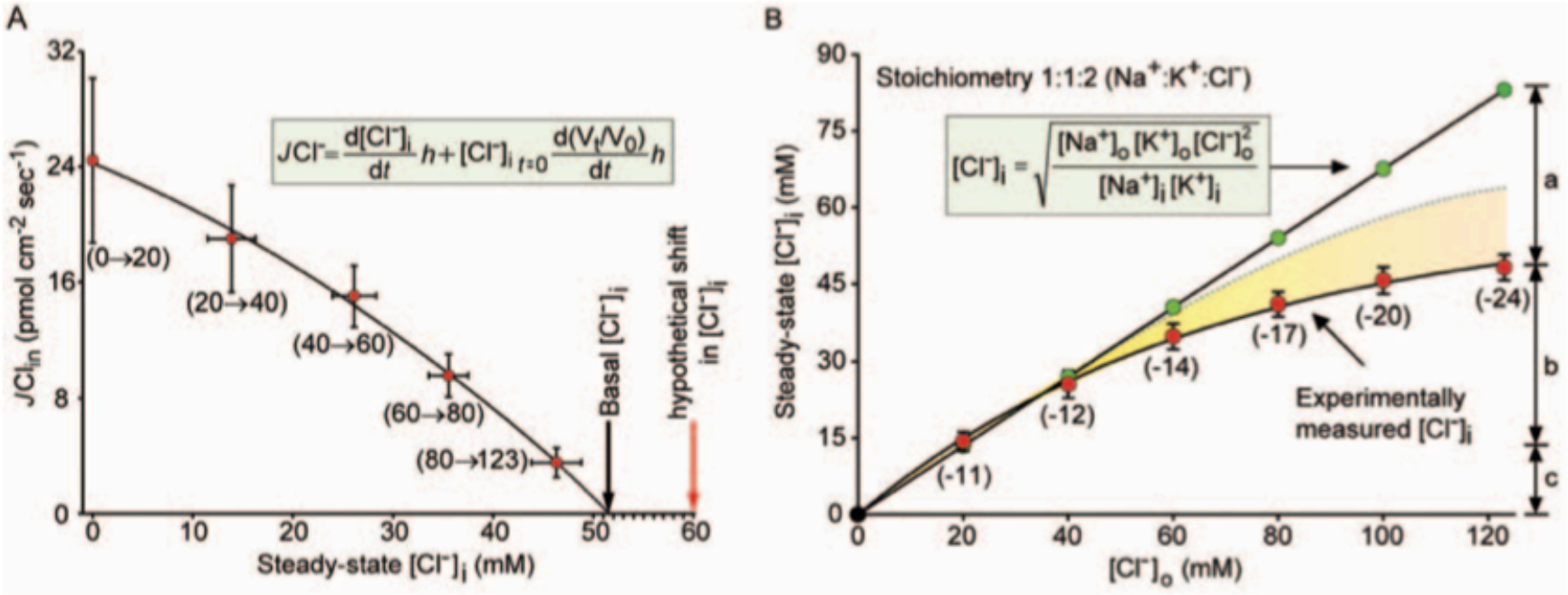

FIGURE 22.9 Intracellular $[Cl^-]$ regulates Cl^- influx through putative negative feedback. **A.** Net Cl^- influx (JCl_{in}) as a function of steady-state $[Cl^-]_i$ for ~20 mM increments in $[Cl^-]_o$. The experimental protocol followed to obtain the data is shown in Fig. 22.8. JCl_{in} was calculated using the boxed equation where: $d[Cl^-]_i/dt$ and $d(V_t/V_o)/dt$ are the initial rates of change in $[Cl^-]_i$ and relative cell water volume, respectively, h is the cell volume-to-surface-ratio (cm) assuming spherical shape. Numbers in parenthesis indicate the increments in $[Cl^-]_o$ in mM (the first number is the initial $[Cl^-]_o$ and the second is the final $[Cl^-]_o$ for each step change in $[Cl^-]_o$). Note that $J\,Cl_{in}$ decreases as $[Cl^-]_i$ increases. Bars on each point are SE. JCl_{in} measured when the external solution was changed from 0 to 20 mM Cl^- (0→20) is the sum of SDC and SIC Cl^- influx. Other points reflect Na^+-dependent "uphill" JCl_{in}. Black arrow indicates the extrapolated $[Cl^-]_i$ (~50 ± 5 mM) at which JCl_{in} becomes negligible. This value is close to the measured basal $[Cl^-]_i$. Red arrow: possible shit in $[Cl^-]_i$ resulting from a change in set point due to a change (a decrease) in Cl^- sensitivity of NKCC or associated regulatory proteins (e.g. kinases). **B.** Steady-state $[Cl^-]_i$ as a function of $[Cl^-]_o$. Green circles denote $[Cl^-]_i$ (calculated from the boxed equation) when NKCC attains thermodynamic equilibrium. NKCC stoichiometry was assumed to be 1:1:2. $[Na^+]_i$ = 10 mM and $[K^+]_i$ = 135 both assumed to be kept constant by the Na^+/K^+ pump. Red circles are actual steady-state $[Cl^-]_i$ measured for various $[Cl^-]_o$ (n = 11). Values in parenthesis correspond to E_{Cl} (in mV). Bracketed arrows: **a**, theoretical range in which $[Cl^-]_i$ could increase by NKCC upregulation. It is the difference between the maximal theoretical $[Cl^-]_i$ if NKCC attained thermodynamic equilibrium (83 mM) and the value measured (48.3±2.5 mM) at physiological $[Cl^-]_o$ (123 mM). This range represents the hypothetical "window" in which $[Cl^-]_i$ could be shifted by changes in the kinetic brake (set point); **b**, range of $[Cl^-]_i$ above electrochemical equilibrium; **c**, range of $[Cl^-]_i$ below electrochemical equilibrium. The dotted gray line and the shadowed area represent a hypothetical shift in set point and therefore in E_{Cl}.

Targeting

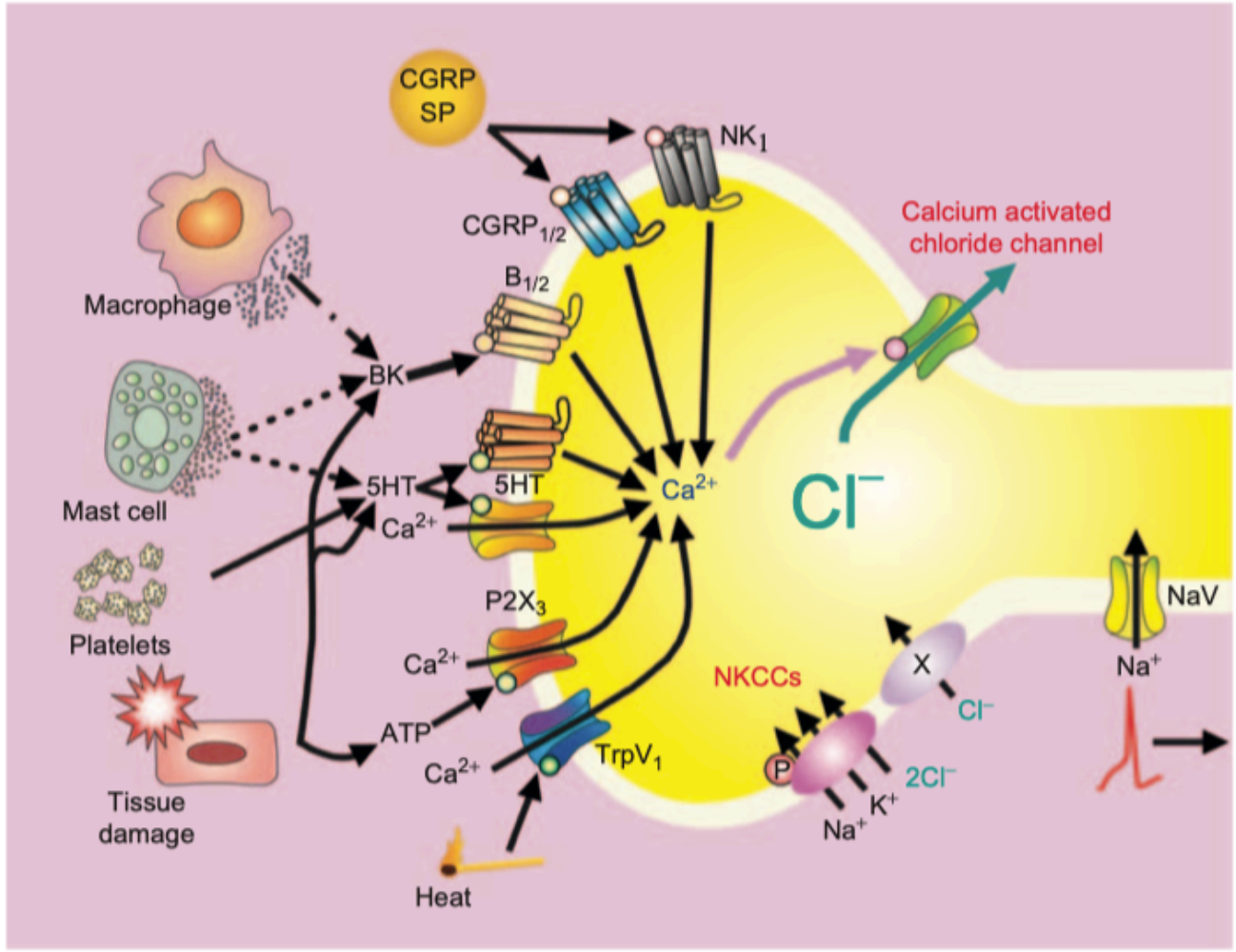

FIGURE 22.10 Schematic representation of the hypothetical processes occurring within a primary afferent nociceptor that leads to spike initiation. We propose that NKCC and other yet to be identified active Cl^- uptake transport systems (X), maintain an outward Cl^- gradient across the nociceptive terminal plasma membrane. This Cl^- gradient plays a key role in producing the nociceptor generator potential, a local depolarization that reaches threshold and initiate an all or none action potential. Nociceptors have receptors for various inflammatory mediators. A common feature of many inflammatory mediators such as serotonin (5HT), bradykinin (BK), ATP or activation of TRPV1 receptor channels is that all of them ultimately increase the concentration of intracellular Ca^{2+} in the nociceptive terminal. The increase in Ca^{2+} triggers a depolarizing Cl^- efflux via Ca^{2+}-activated Cl^- channels. When the depolarization reaches threshold, an action potential is generated.

Targeting

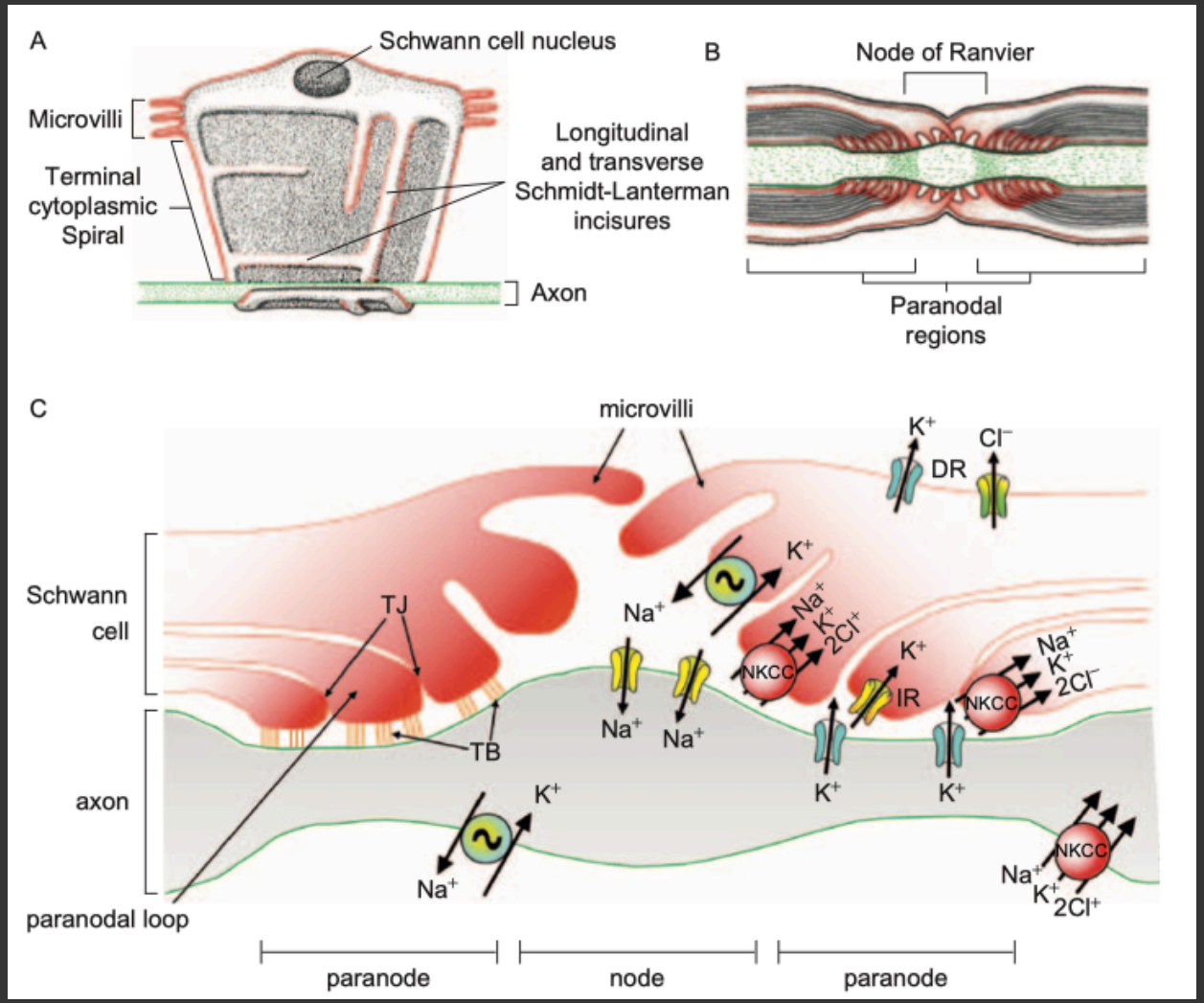
A
Schwann cell nucleus
Microvilli
Terminal cytoplasmic Spiral
Longitudinal and transverse Schmidt-Lanterman incisures
Axon
B
Node of Ranvier
Paranodal regions
C
microvilli
Schwann cell
axon
paranodal loop
TJ
TB
DR
IR
NKCC
paranode
node
paranode

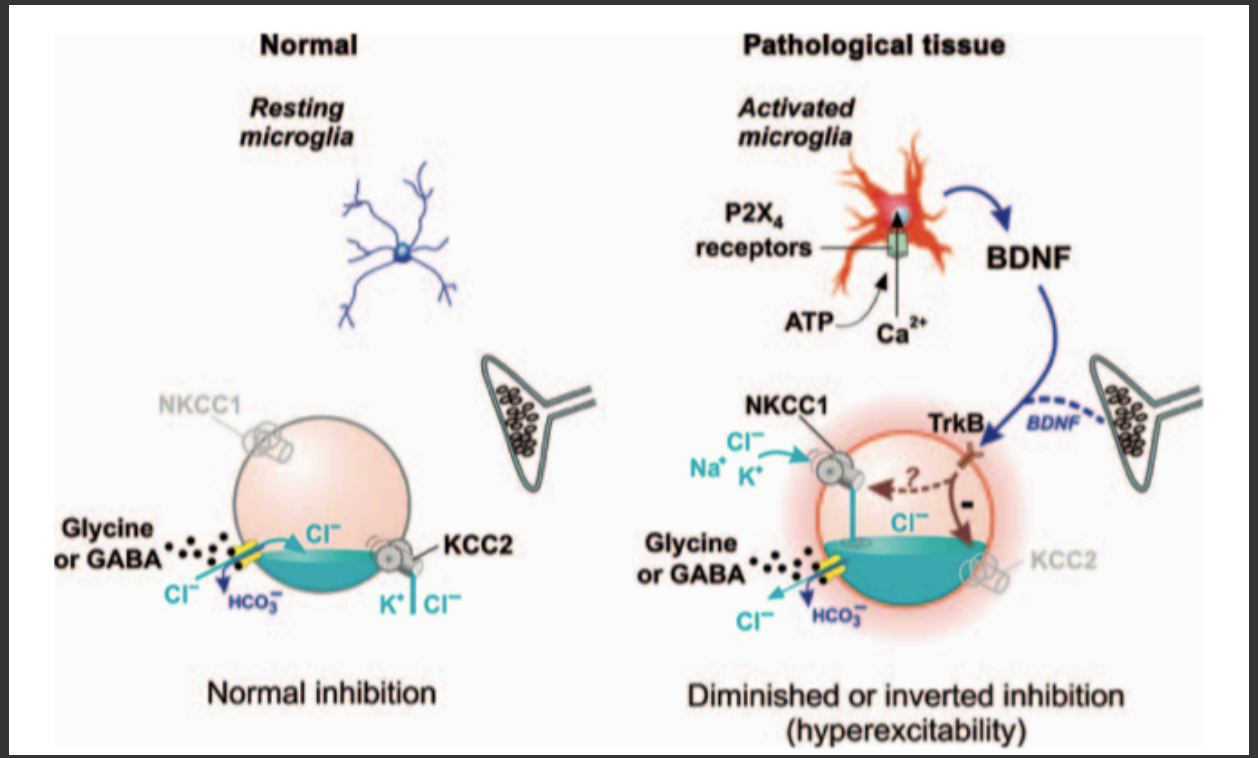
Normal
Resting microglia
NKCC1
Glycine or GABA
KCC2
Normal inhibition
Pathological tissue
Activated microglia
P2X4 receptors
ATP
Ca2+
BDNF
TrkB
Diminished or inverted inhibition (hyperexcitability)

Options

- Would modulation of some other channel lead to presynaptic inhibition?
  - NKCC
  - NKCC1
  - 5HT
  - $P2X_3$
  - $P2X_4$
  - CGRPSP